Acta Cryst. (1998). B54, 231–239

Comparison of Experimental and Theoretical Structure Amplitudes and Valence Charge Densities of GaAs

J. Stahn, M. Möhle and U. Pietsch*

Institute of Physics, University of Potsdam, Am Neuen Palais 10, D-14469 Potsdam, Germany.
E-mail: upietsch@rz.uni-potsdam.de

(*Received 16 June 1997; accepted 20 October 1997*)

Abstract

The current best sets of X-ray structure amplitudes for GaAs, gallium arsenide, are completed by highly precise data recorded at $0.50 < \sin\theta/\lambda < 1.35$ Å^{-1}. For the strong reflections the required accuracy of $\Delta F/F \leq 1\%$ was realized by the use of *Pendellösung* measurements at $\lambda = 0.30$ Å, recording the integral intensities as a function of the effective thickness from ~500 μm thick GaAs wafers. Additionally, several weak reflections were determined from their integral intensities within the kinematic limit at wavelengths $\lambda = 0.3$, 0.56 and 0.71 Å. From these data individual Debye–Waller factors for gallium and arsenic were determined using the model of independent spherical atoms [$B_{Ga} = 0.666\ (4)$ and $B_{As} = 0.566\ (4)$ Å^2]. The extended set of experimental structure factors now available is compared with those obtained by *ab initio* solid-state Hartree–Fock (HF) and density functional (DF) calculations. Therefore, the theoretical data were adapted to room temperature using the experimentally evaluated Debye–Waller factors and the model mentioned above. The valence and difference charge densities obtained from experimental and theoretical data show the expected charge accumulation between nearest neighbours slightly shifted towards the arsenic site. The disagreement remaining between the experimental and theoretical data, on the one hand, and between those of both *ab initio* methods, on the other hand, are of the same order of magnitude.

1. Introduction

The most characteristic feature of the valence charge density of GaAs is a charge density accumulation between next neighbours slightly shifted towards the As atom. This is explained by the constructive overlap of bonding orbitals and the charge transfer between nearest neighbours. As shown recently (Pietsch & Hansen, 1996), only a few of the charge density maps calculated from different data sets of X-ray structure amplitudes $|F_\mathbf{h}|$ published until now (Levalois & Allais, 1986; Saravanan *et al.*, 1992; Stevenson, 1994) are in qualitative agreement with this theoretical prediction.

To check this feature one has to determine the valence charge density (VCD) using structure factors with an accuracy greater than 1%. This accuracy requires measuring procedures which allow a precise data reduction, that means experiments which fit either the kinematical or the dynamical limit of X-ray scattering theory.

Owing to the proximity of gallium to arsenic in the periodic table, the zinc blende structure crystal GaAs exhibits Bragg reflections of very different scattering power. For small $\sin\theta/\lambda$ the moduli of the X-ray structure factors $F_\mathbf{h}$ of the class $h + k + l = 4n$ and $4n \pm 1$ are of the order of 100. Then the extinction length is smaller than the absorption length in the case of almost perfect crystals. The conventional techniques of structure analysis prevent the determination of highly precise $|F_\mathbf{h}|$, because the integral intensities are strongly affected by secondary extinction. To overcome this problem experiments have been performed which can be solely interpreted by the dynamical theory of X-ray diffraction. For example, the detection of *Pendellösung* oscillations (Kobayshi *et al.*, 1988) and the measurement of the angular half-width of Bragg peaks (Matsushita & Hayashi, 1977). On the other hand, the class $h + k + l = 4n + 2$ Bragg reflections are weak ($|F_\mathbf{h}| < 6$) and their integral intensities are controlled solely by the absorption length. This justifies the use of conventional techniques, *i.e.* collecting the integral intensity of a Bragg reflection, taking care that *Umweganregung* can be ruled out (Pietsch, 1981; Bilderback, 1975; Stevenson, 1996).

In this work we present *Pendellösung* measurements for the strong reflections and conventional techniques for weak reflections in order to complete the best data sets so far by high-order reflections (Matsushita & Hayashi, 1977; Pietsch *et al.*, 1986).

Comparison of experimental and theoretical structure factors can be performed in two ways. A comparison of $|F_\mathbf{h}|$ has the advantage of being close to the experiment. A clear disadvantage of this method is that one cannot distinguish whether the differences result from statistical errors in the measurements or from incorrect predictions of the theory concerning charge transfer or charge accumulations, for example.

An instructive picture of the charge density is obtained by Fourier transformation of $F_{\mathbf{h}}$. Here the bonding effects are visualized, especially by calculating the difference charge densities (DCD). Since the data set is limited in reciprocal space, the appearance of ghost peaks hinders the production of a physically correct density map.

In any case it is necessary to have experimental and theoretical $|F_{\mathbf{h}}|$ on a similar level. This requires the reduction of experimental structure factors for anomalous dispersion and the rescaling of theoretical data to room temperature (Pietsch & Hansen, 1996). Owing to the non-centrosymmetry of the zinc blende structure, this requires the use of a charge density model. This should be as simple as possible, thus all corrections and fits we made (as the reduction of the Debye–Waller factors and their introduction into theoretical data) were based on the model of superposed free spherical atoms or quasi-atoms adapted to the crystal structure. This is a good approximation for reflections with $\sin\theta/\lambda > 0.5$ Å^{-1}.

In the next two sections the measurements and the data reduction will be described. The processing of the theoretical data is explained in §5, followed by comparison and discussion of the VCD's and DCD's in §6 and §7.

2. *Pendellösung* measurements

According to Kato (1968), the integral intensity R for a set-up in symmetric Laue geometry oscillates as

$$R = (\pi/2)|F_{\mathbf{h}}/F_{\bar{\mathbf{h}}}| \exp[-\mu t/\cos\theta\cos\Phi] \times |B| \int_{-1}^{1} |J_0[B(1-x^2)^{1/2}]|^2 \mathrm{d}x \quad (1)$$

with

$$B = (r_e/V)\{[t\lambda(F_{\mathbf{h}}F_{\bar{\mathbf{h}}})^{1/2}]/\cos\theta\cos\Phi\}, \quad (2)$$

in which R depends on the product of wavelength, structure amplitude and effective sample thickness, $\lambda F_{\mathbf{h}} t$, respectively. J_0 is the zero-order Bessel function. μ is the absorption coefficient, r_e the classical electron radius and V the volume of the elementary cell. θ and Φ are the Bragg and tilt angles, respectively. The variation of R as a function of the effective sample thickness t was realized by rotating the crystal wafer by discrete angular steps, $\Delta\Phi$, around the scattering vector (inclination method).

The experiments were performed at the four-circle diffractometer of the D3 beamline at HASYLAB. The temperature was 297 ± 1 K. The spot size on the sample was ~1 mm^2. The use of a Si(111) double-crystal monochromator led to an energy resolution of the incident beam greater than $\Delta E/E = 10^{-4}$ for radiation with wavelength $\lambda = 0.3$ Å. This wavelength was chosen in order to reduce absorption. A further decrease of the wavelength led to the disappearence of oscillations. We assume that point defect clusters and growth striations prevent the creation of the dynamical wavefield in the crystal. For $\lambda = 0.3$ Å oscillation behaviour appeared only on sample areas which were not perturbed by dislocations. Owing to the etch pitch density (e.p.d. = density of dislocations on the surface) of ~500 cm^{-2}, no beating effects were detected for reflections other than those given in Table 1.

Table 1. *Real F' and imaginary F'' parts evaluated by Pendellösung measurements and their comparison with those obtained by the superposition of spherical atoms F^{sph} using temperature factors given in §4 and anomalous dispersion contributions given in Table 2*

hkl	$\sin\theta/\lambda$	F'	F''	$F^{sph\prime}$	$F^{sph\prime\prime}$
440	0.500	112.55	3.22	110.80	2.57
620	0.559	97.45	3.17	96.89	2.47
444	0.613	86.33	2.65	85.39	2.38
553	0.679	52.57	1.78	51.64	1.61
800	0.708	68.81	2.85	68.25	2.21
660	0.751	62.62	2.50	61.58	2.12
664	0.830	51.99	2.16	50.89	1.96
880	1.010	35.64	2.08	34.54	1.62
777	1.072	22.06	1.39	20.97	1.06

The surface orientations of the GaAs wafers were [110] and [100] and the thicknesses $t = 519$ (2) and $t = 481$ (2) μm, respectively. t was determined using a contact method with an accuracy of ~0.2%. *Pendellösung* could be observed for 9 reflections in the range $0.50 < \sin\theta/\lambda < 1.07$ Å^{-1} for tilt angles Φ between −60 and +60°.

Fig. 1 shows several *Pendellösung* curves. From these the $F_{\mathbf{h}}$ were obtained by least-squares fits of (1). The results are presented in Table 1. The imaginary F'' are due to anomalous dispersion. The correction for dispersion was performed using $\Re e(F_{\mathbf{h}}F_{\bar{\mathbf{h}}})^{1/2} \simeq \Re e(F_{\mathbf{h}})$

$$F_{\mathbf{h}} \simeq \Re e(F_{\mathbf{h}}F_{\bar{\mathbf{h}}})^{1/2} - 4(f'_{Ga}T_{Ga} + f'_{As}T_{As}) \quad (3)$$

for the strong reflections and

$$F_{\mathbf{h}} \simeq \left(\Re e[(F_{\mathbf{h}}F_{\bar{\mathbf{h}}})^{1/2}]^2 - \Delta_r^2 - \{\Delta_i^4/4\Re e[(F_{\mathbf{h}}F_{\bar{\mathbf{h}}})^{1/2}]^2\}\right)^{1/2} \quad (4)$$

for the medium ones. With

$$\Delta_r = 16(2f^{sph}_{Ga}f'_{Ga} + f'^2_{Ga} - f''^2_{Ga})T^2_{Ga} + 16(2f^{sph}_{As}f'_{As} + f'^2_{As} - f''^2_{As})T^2_{As}$$

$$\Delta_i = 32(f^{sph}_{Ga} + f'_{Ga})f''_{Ga}T^2_{Ga} + 32(2f^{sph}_{As} + f'_{As})f''_{As}T^2_{As}.$$

The dispersion parameters f' and f'', which are used for all corrections, are displayed in Table 2. The structure amplitudes of the free atoms f_i^{sph} were taken from

International Tables for Crystallography (1995, Vol. C). The temperature factors $T_i = \exp[-B_i \sin^2\theta/\lambda^2]$ contain the Debye–Waller factors B_{Ga} and B_{As}, as evaluated by the procedure explained in §4. The structure factors after correction by (3) and (4) are given in Table 4.

3. Weak reflections

To obtain accurate data, even for high-order Miller indices, three sets of reflections were collected at HASYLAB using wavelengths λ = 0.3, 0.56 and 0.71 Å, measuring the integral intensities in Bragg geometry. To avoid *Umweganregung*, Ψ scans around the normal of the reflecting lattice plane were performed.

To deduce the weak structure factors the measured intensities $R_{\mathbf{h}\lambda T}$ were normalized and corrected for polarization, absorption and dispersion. Since the dispersion parameters f' and f'' are defined as atomic

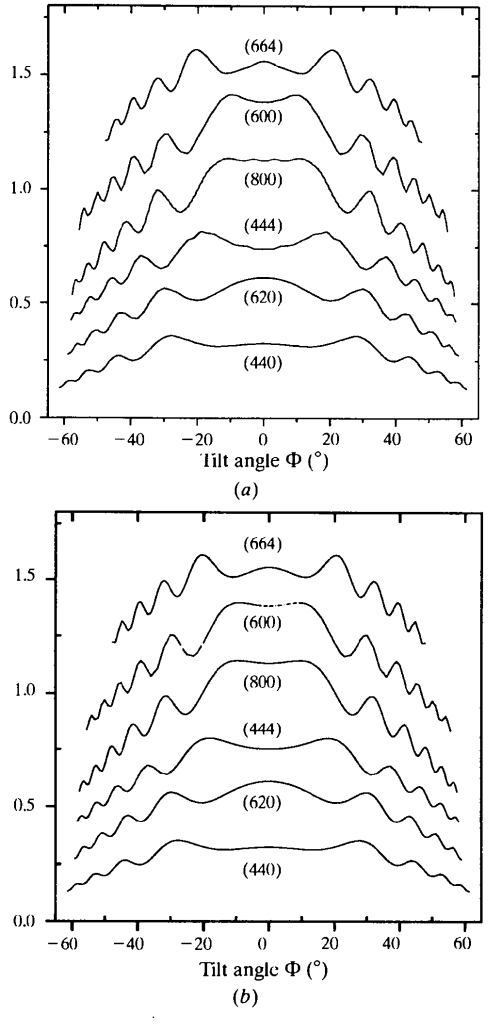

Fig. 1. Several (*a*) experimental and (*b*) fitted curves displaying *Pendellösung*. For clarity, they are multiplied by a suitable factor.

Table 2. *Factors for the dispersion correction used in (5)*

The factors for 0.71 and 0.56 Å are taken from *International Tables for Crystallography* (1995, Vol. C) and for 0.30 Å by Creagh (1996) and Cromer & Liberman (1970).

λ (Å)	f'_{Ga}	f''_{Ga}	f'_{As}	f''_{As}
0.71	0.2307	1.6083	0.0499	2.0058
0.56	0.3179	1.5089	0.2758	1.3314
0.30	0.1684	0.330	0.1940	0.420

quantities, they are also affected by thermal smearing. This is why one has to introduce a suitable model which allows the extraction of $|F_{\mathbf{h}}|$. Considering absorption, dispersion and thermal effects (Debye model, independent thermal motion of the atoms in a spherical harmonic potential), $F_{\mathbf{h}\lambda T}$ in the spherical atom approximation is given by

$$F_{\mathbf{h}\lambda T} = 4(f_{Ga\mathbf{h}} + f'_{Ga\lambda} + if''_{Ga\lambda})T_{Ga\mathbf{h}} + c4(f_{As\mathbf{h}} + f'_{As\lambda} + if''_{As\lambda})T_{As\mathbf{h}} \quad (5)$$

$$c = i^{h+k+l} = \begin{cases} 1 & \text{for } h+k+l = 4n \\ i & \text{for } h+k+l = 4n+1 \\ -1 & \text{for } h+k+l = 4n+2 \\ -i & \text{for } h+k+l = 4n-1, \end{cases}$$

where c describes the phase relation between the Ga and As sublattices. $f_{Ga\mathbf{h}}$ and $f_{As\mathbf{h}}$ are the relativistic form factors of the free atoms as given by Su & Coppens (1994). $f'_{i\lambda}$ and $f''_{i\lambda}$ and are taken from Table 2.

$|F_{\mathbf{h}\lambda T}|$ is obtained from the measured quantity $R_{\mathbf{h}\lambda T}$ using

$$R_{\mathbf{h}\lambda T} = s^2 PL|F_{\mathbf{h}\lambda T}|^2, \quad (6)$$

where $L = 1/\sin 2\theta$ is the Lorentz factor and P is the polarization of the incoming beam. The absorption correction included in the scaling factor s was performed with the assumption that the crystal thickness could be treated as being semi-infinite. For λ = 0.3 Å an estimation of the influence of the thermal diffuse scattering (TDS) according to Willis (1969) gave the dependence $R_{TDS} = (1 + 6.7 \times 10^{-3}\sin^2\theta/\lambda^2\,\text{Å}^2)R$. For the other wavelengths the effect is even smaller. This means that TDS is negligible for the presented data.

For weak reflections the influence of extinction was estimated assuming that the measured reflectivity had to be treated within dynamical theory: $|R^{meas}| := |R^{dyn}|$ (worst case). In Table 4 the $|R^{meas}|$ values are displayed for λ = 0.56 Å. The deviations between $|R^{kin}|$ and $|R^{meas}|$ are smaller than 1–2%. This means that the maximum correction of the structure amplitude by extinction would not exceed the measurement error. Therefore, no extinction correction is performed.

The parameters s and P in (6) were evaluated by a least-squares fit using $F_{\mathbf{h}\lambda T}$ obtained from (5) for reflections with $\sin\theta/\lambda > 0.5$ Å^{-1}. As the temperature

factors B_{Ga} and B_{As} are not known exactly (Pietsch & Hansen, 1996), they have to be included in the fitting procedure (see below).

The rescaled structure factor moduli were corrected for anomalous dispersion with

$$|F_{\mathbf{h}}| = [|F_{\mathbf{h},\text{incl.disp.}}|^2 - 16(f''_{Ga}T_{Ga} - f''_{As}T_{As})^2]^{1/2} + 4(f'_{Ga}T_{Ga} - f'_{As}T_{As}). \quad (7)$$

The results are presented in Table 5, together with calculated structure factors.

The dispersion corrections [(3), (4) and (5)] are based on the model of superposition of spherical atoms, neglecting charge transfer and bond charges. This arbitrary subdivision gives rise to an error in the derived valence charge density. For strong and medium reflections, and for weak reflections with $\sin\theta/\lambda > 0.5$ Å^{-1} this has no influence. Weak reflections with $\sin\theta/\lambda < 0.5$ Å^{-1} are mainly affected by a phase factor error.

For most of the measured reflections the scattering phases needed for the Fourier synthesis are taken from solid-state Hartree–Fock calculations (see later). This is an acceptable approximation because the deviations of the scattering phases caused by the rearrangement of the electron density relative to the free atoms are small in both cases.

The phase of the 222 reflection was determined using the bond-charge model (Pietsch & Hansen, 1996). For reflections with $hkl = 0$ the phase is given solely by symmetry.

4. Debye–Waller factors

Owing to the different values of factor c in (5), there is no overall Debye–Waller factor for all reflections of GaAs (and all other zinc blende structure crystals). While the amount of strong reflections decreases with rising temperature, several weak reflections exist which increase since $B_{As} < B_{Ga}$.

The Debye–Waller factors, obtained by least-squares fit to the experimental data *via* (5), are $B_{Ga} = 0.666$ (4) and $B_{As} = 0.566$ (4) Å^2. They refer to $T = 287.15$ K and are adapted to T_{exp} supposing a linear temperature dependence of $B_T = B_{287.15\,K}T/287.15$ K.

As shown in the residual plots in Fig. 2, the least-squares fit including the strong reflections is sensitive only for the sum $B_{Ga} + B_{As}$, while the same procedure for the weak reflections is sensitive to their difference. The intersection of both valleys coincides with the Debye–Waller factors obtained by the fit, including the whole data set within the error range.

5. Theoretical structure factors

The theoretical structure factors used in this work are based on Hartree–Fock and density functional calculations. The former were obtained with the *ab initio* solid-state Hartree–Fock program *CRYSTAL* 92 (Dovesi *et al.*, 1992), $F_{\mathbf{h}}^{HF}$. The basis set was obtained from 976-311d51G atomic basis sets (Towler, 1996) by omitting the outermost *s*- and *p*-like functions (which led to linear dependences) and reoptimizing the valence functions with respect to the total energy.

Calculations within the density functional theory ($F_{\mathbf{h}}^{DF}$) were performed by Blaha using the program *WIEN*95 (Blaha, 1996).

In contrast to the experimental data, the theoretical data are not affected by thermal smearing. A deconvolution of experimental F would lead to an increased uncertainty for high-order structure factors. Since we assume that the interesting features of the VCD are mainly described by low-order reflections and since these are weakly affected by temperature, it seems profitable to rescale the theoretical data to room

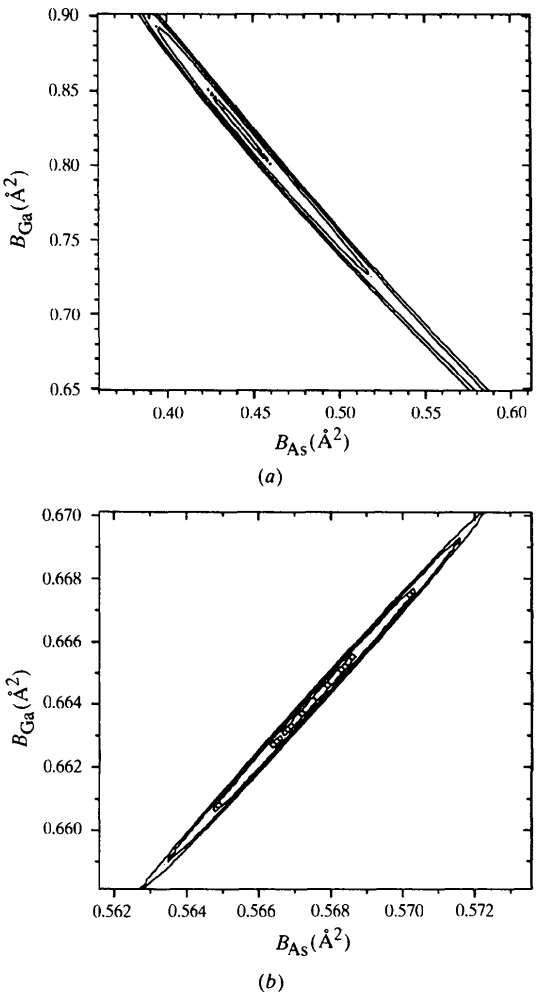

Fig. 2. Contour plots of $\Sigma(F^{exp} - F^{theo})/F^{exp}$, F^{theo} calculated by (5) as a function of B_{Ga} and B_{As} for the class of (*a*) strong and (*b*) weak reflections.

temperature. In this way both structure factors and electron densities can be compared.

Since Ga and As atoms in GaAs show different dependencies on the temperature, the electron density and therefore the structure factors need to be separated into Ga and As contributions. Owing to the non-centrosymmetry of the zinc blende structure, this again is impossible without model assumptions. One possible method has been described by Lichanot *et al.* (1996), who modified the Gauss exponents of the basis functions of the Hartree–Fock calculation. Since these basis functions are centred at the atomic positions, the separation is easy.

We used a different approach: The atomic Debye–Waller factors were obtained from experimental data using the model of the superposition of spherical atoms (§4). These factors are introduced into the theoretical data using the same formulae. Now f_{Ga} and f_{As} in (5) are interpreted as the structure factors of the corresponding sublattices (f' and f'' are zero). Both structure factors are affected by the charge transfer and other interactions with each other. Due to the lack of an inversion centre f_i are in general complex quantities.

Owing to the phase relation between the sublattices, which is represented by c in (5), there are four groups of structure factors. By adding or subtracting strong ($c = 1$: $F_{\mathbf{h}}^{s}$) and weak ($c = -1$: $F_{\mathbf{h}}^{w}$) structure factors one obtains

$$f_{Gah} = (1/8)[F_{\mathbf{h}}^{s} + F_{\mathbf{h}}^{w}], f_{Ash} = (1/8)[F_{\mathbf{h}}^{s} - F_{\mathbf{h}}^{w}].$$

Analogously for the other two groups with $c = i$: $F_{\mathbf{h}}^{+}$ and $c = -i$: $F_{\mathbf{h}}^{-}$

$$f_{Gah} = (1/8)[F_{\mathbf{h}}^{+} + iF_{\mathbf{h}}^{-}], f_{Ash} = (1/8)[F_{\mathbf{h}}^{+} + iF_{\mathbf{h}}^{-}].$$

For a given set of *hkl* only one of the structure factors, $F_{\mathbf{h}}^{s}$ or $F_{\mathbf{h}}^{w}$, exists. The missing values are interpolated within their group. This approach leads to reasonable results since the behaviour of $F_{\mathbf{h}}$ is sufficiently smooth. The interpolation was carried out using the method of Lagrange, as published in *International Tables for Crystallography* (1995, Vol. C). By this method a possible change of the scattering phases induced by thermal vibration of the atoms is neglected.

For the other reflections the separation is much easier: the real part of $F_{\mathbf{h}}$ is f_{Ga}, the imaginary part f_{As}.

In addition to the mentioned temperature correction the anharmonicity of the potential of atomic movement was taken into account by multiplying

$$[1 + i(B_i/4\pi a_o)^3 \beta_i(hkl/k_B T)]$$

with both items in (5), using the relation $\beta_{Ga} \simeq -\beta_{As}$. β_{As} was determined by Pietsch *et al.* (1993) from the Bijvoet relation of GaAs $666/\bar{6}\bar{6}\bar{6}$ to -1.75×10^{-19} J Å^{-3} (see also Stevenson, 1996).

Table 3. *Strong and medium reflections for GaAs*

Those labelled with *a* and *b* were measured with the *Pendellösung* method at T = 297.15 and 299.15 K, respectively (Möhle, 1997). Reflections labelled *c* were measured by Matsushita & Hayashi (1977) at T = 299.15 K. The experimental data are corrected for dispersion. The theoretical data are adapted to room temperature as described in §5.

hkl		F^{exp}	F^{HP}	F^{DF}	F^{sph}
111	*c*	154.91	153.52	152.90	152.82
220	*c*	180.70	182.11	182.08	182.91
311	*c*	118.37	118.98	120.03	119.77
400	*c*	150.48	150.48	150.06	150.94
331	*c*	100.77	100.40	99.67	100.27
422	*c*	128.43	128.24	127.95	128.18
333	*c*	85.11	85.77	84.65	85.70
511	*c*	85.64	85.83	84.97	85.78
440	*c*	110.50	110.64	110.59	110.67
440	*a*	111.30	110.75	110.71	110.78
620	*a*	96.26	96.669	6.80	96.85
444	*c*	85.10	85.16	85.35	85.36
444	*b*	85.18	85.16	85.35	85.36
553	*b*	51.60	51.48	52.19	51.56
800	*a*	67.75	67.80	68.27	68.07
660	*a*	61.60	61.16	61.66	61.56
664	*b*	51.01	50.52	51.03	50.86
880	*a*	34.86	34.28	34.68	34.52
777	*a*	21.56			

Table 4. *To estimate the maximum possible influence of extinction the reflectivities of weak reflections measured at λ = 056 Å were treated in terms of the dynamical theory ($|R^{meas}| = |R^{dyn}|$)*

The reflections are compared with corresponding ones calculated by kinematical theory, $|R_{\mathbf{h}}^{kin}|$ (Zachariasen, 1967).

hkl	sin θ/λ	$\lvert R_{\mathbf{h}}^{meas}\rvert$	$\lvert R_{\mathbf{h}}^{kin}\rvert$
222	0.306	62.7	63.9
$\bar{2}\bar{2}2$	0.306	70.7	72.0
420	0.395	75.3	77.1
442	0.531	80.4	83.2
600	0.531	81.1	82.5
622	0.586	79.4	81.4
640	0.638	74.5	76.2
644	0.729	66.4	67.7
820	0.729	66.4	67.7
662	0.771	61.0	62.0
842	0.810	58.0	58.9
860	0.884	50.6	51.2
864	0.952	44.5	45.0
10,40	0.952	44.7	45.2
882	1.016	40.1	40.5
10,62	1.046	37.9	38.2
886	1.132	33.2	33.5
10,80	1.132	33.0	33.3
10,66	1.160	31.9	32.1
10,84	1.186	31.0	31.2
10,10,2	1.263	27.9	28.1
10,10,6	1.358	25.1	25.2

6. Results

The corrected experimental structure factors are dispayed in Tables 3 and 5 compared with those obtained by Hartree–Fock and density functional

Table 5. *Weak reflections of GaAs*

The first experimental data set was measured at λ = 0.30 Å, T = 297.65 K, the second at λ = 0.56 K, T = 299.15 K and the third at λ = 0.71 Å, T = 299.15 K. They were treated within the kinematical limit of scattering theory and are corrected for dispersion. The theoretical data were adapted to room temperature (see §5).

hkl	$F^{exp}_{0.30}$	$F^{exp}_{0.56}$	$F^{exp}_{0.71}$	F^{HF}	F^{DF}	F^{sph}
200	6.34			6.29	6.26	5.81
222	5.67	5.50	5.57	5.32	5.65	5.50
420	6.64	6.23	6.28	6.16	6.30	6.34
442		6.71	6.78	6.80	6.72	6.79
600		6.65	6.75	6.78	6.70	6.78
622	6.88	6.56	6.55	6.61	6.51	6.59
640		6.13	6.26	6.23	6.19	6.27
644		5.42	5.50	5.47	5.44	5.49
820		5.42	5.44	5.47	5.43	5.49
662		4.95	5.11	5.07	5.05	5.10
842	4.87	4.69	4.72	4.70	4.69	4.73
860	4.22	4.06	4.10	4.03	4.06	4.08
10,00	4.16			4.04	4.07	4.08
864		3.54	3.54	3.51	3.56	3.55
10,40		3.55	3.54	3.51	3.55	3.55
882	3.19	3.16	3.16	3.10	3.15	3.13
10,62		2.97	2.97	2.93	2.98	2.96
886	2.60	2.58	2.57	2.53	2.59	2.57
10,80		2.56		2.52	2.57	2.55
10,66		2.47	2.45	2.43	2.48	2.46
10,84		2.40	2.34	2.32	2.37	2.36
12,60	2.35			2.32	2.37	2.35
14,00	2.19			2.16	2.20	2.19
10,10·2		2.14		2.09	2.13	2.11
12,82	2.03			2.02	2.06	2.05
10,10·6	1.90	1.91		1.87	1.90	1.89
14,62	1.86			1.85	1.88	1.88
12,10,4	1.74			1.72		1.74
14,66	1.68			1.67		1.70
16,42	1.65			1.62		1.64
14,10,2	1.51			1.50		1.52
12,10,8	1.48			1.49		1.51
16,82	1.41			1.39		1.41
18,00	1.41			1.39		1.41
14,12,4	1.21			1.26		1.27
18,62	1.23			1.22		1.23
18,80	1.08			1.12		1.13
20,20	0.99			1.06		1.03
16,10,8	0.99			1.02		1.03
22,00	0.80			0.78		0.80
22,80	0.61			0.60		0.62

calculations and by the superposition of spherical atoms (F^{HF}, F^{DF} and F^{sph}). The theoretical data are adapted to room temperature. The experimental data set is expanded by several reflections measured by Matsushita & Hayashi (1977).

To realize the importance of certain reflections in describing the charge density in the bonding region a series of VCD's was generated based on the following data sets: For Fig. 3(*a*) all the experimental structure factors given in Tables 3 and 5 (column $F^{exp}_{0.56}$) were used. The corresponding F^{HF}'s were used to generate Fig. 3(*b*). Fig. 4(*a*) is based on an extended set of F^{HF}'s complete up to the cut-off point of $\sin\theta/\lambda$ = 2.5 Å^{-1}. Fig. 4(*b*) was obtained by superposition of spherical atoms (same reflections as above), where the reflections 222, 420, 111 and 311 were substituted by bond-charge-dependent experimental reflections. Fig. 5 is obtained by Fourier transforming these four experimental structure factors.

All DCD's and VCD's were obtained by subtracting the spherical atom form factors or their core contributions given by Su & Coppens (1994).

If the data set is incomplete negative regions may appear in the VCD. For the same reason the core regions are not described correctly whenever high-order reflections are missing.

7. Discussion

As can be seen in Tables 3 and 5, discrepancies between the experimental, on the one hand, and the HF and DF structure amplitudes, on the other hand, are very small. The differences do not exceed 1% for the strong and medium structure factors and up to 5% for the weak ones. 1% is the error range of the experimental values and the Debye–Waller factors.

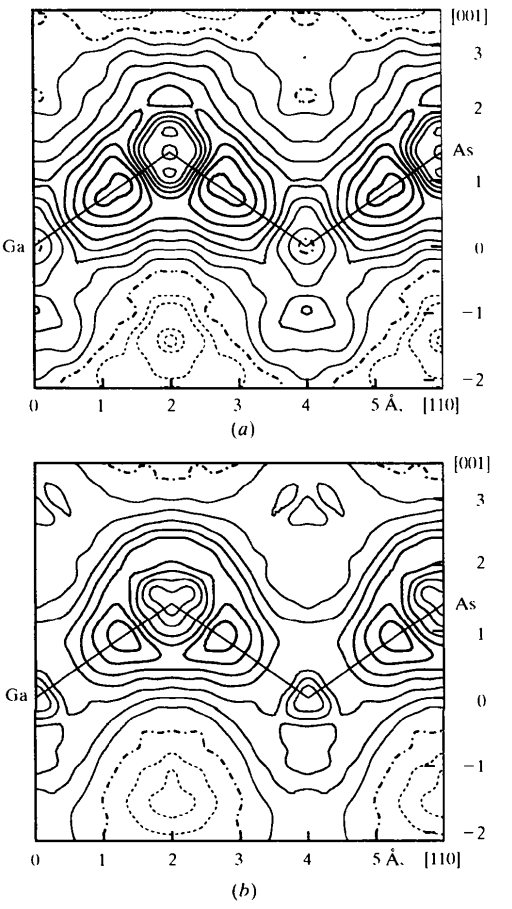

Fig. 3. VCD, calculated from (*a*) experimental and (*b*) theoretical structure factors (Tables 3 and 5) after subtraction of the core contributions. The distance between the contour lines is 0.075 e Å^{-3}, negative areas are dashed.

Generally, the difference between $|F^{HF}|$ and $|F^{exp}|$ is smaller than between $|F^{DF}|$ and $|F^{exp}|$ for the strong and medium reflections, while for the weak ones the situation is reversed. For both groups of structure factors $|F^{HF}|$ is significantly smaller than $|F^{DF}|$ for high-order reflections.

The F^{sph} are close to F^{HF} and F^{DF} for high-order reflections. This means that the Debye–Waller factors, determined as fit parameters of R to F^{sph}, are also fit parameters for F^{HF} and F^{DF}. A comparison of pairs of structure factors with equal $\sin\theta/\lambda$, but different indices (442 and 600, 644 and 820, 864 and 10,40, and 886 and 10,80) shows that the influence of anharmonicity is very small. This is in agreement with Stevenson (1994).

The other way to compare experimental and theoretical predictions is based on inspecting VCD's. Owing to the incomplete and limited ($\sin\theta/\lambda < 1.2$ Å) Fourier series only the interatomic regions can be used for discussion.

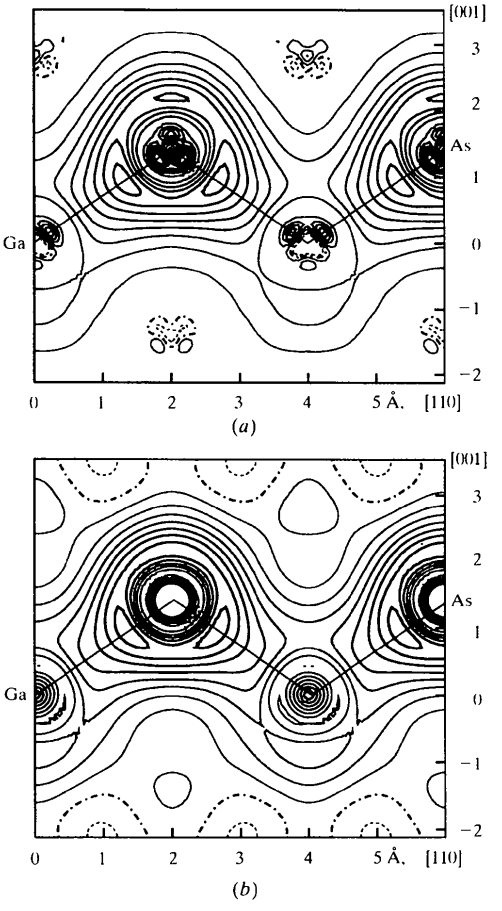

Fig. 4. VCD, calculated from a set of F^{HF} complete up to the cut-off $\sin\theta/\lambda = 2.5$ Å^{-1} (*a*), and from a corresponding set of F^{sph} except for the structure factors 222, 420, 111 and 311, which were determined experimentally (*b*). The distance between the contour lines is 0.075 e Å^{-3}; negative areas dashed.

Figs. 3 and 6 show that the position of the charge accumulation between Ga and As is shifted towards the As site. This occurs in (*a*) the experimental and (*b*) the theoretical (HF) VCD, but HF gives a lower maximum closer to the As site. This indicates that the ionicity of the bond is overestimated by the HF calculation, as implemented in *CRYSTAL*92 (Dovesi *et al.*, 1992) at the cost of covalent bonding. This is also shown in Fig. 7, which displays cuts through the VCD's along the nearest neighbour connection line.

Comparing the VCD's calculated from the limited set of 38 structure factors (Fig. 3*b*), on the one hand, and an extended data set (Fig. 4*a*, both HF), on the other hand, leads to the conclusion that the missing experimental structure factors give rise to more negative areas in the density plots. However, the interesting features such as position, shape and height of the charge accumulation are not affected.

If the set of experimental structure factors consists only of 222, 420, 111 and 311 Fig. 5 results. These bond-charge-dependent reflections seem to be sufficient to describe the covalent part of the bonding between Ga and As. The same conclusion can be obtained by comparing the almost complete VCD's calculated with HF theory (Fig. 4*a*) and by the superposition of spherical atoms, except for afore-mentioned four reflections (Fig. 4*b*).

8. Conclusions

The features of the VCD of GaAs such as charge transfer and covalent bonding are mainly described by a very small number of structure factors, namely 200, 222, 420, 111 and 311. It is therefore possible to obtain the actual VCD by Fourier transformation of a mixed set of structure factors containing the five mentioned measured reflections and theoretical structure factors (up to a certain cut-off) adapted to room temperature.

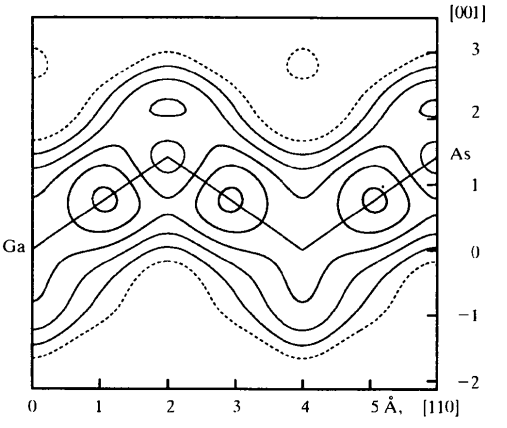

Fig. 5. Electron density calculated by Fourier transformation of the four experimental structure factors 222, 420, 111 and 311. Contours as in Fig. 3.

An extension of the set of F^{exp} does not lead to a more instructive VCD, but adds experimental noise introduced by unavoidable errors of measurement. The high-order reflections are still necessary to determine the Debye–Waller factors.

Most uncertainties in the experimental data result from the data reduction, which always requires model assumptions. This means that the limitation in comparing theory and experiment is not given by a lack of experimental accuracy, but by insufficient theoretical concepts. We therefore assume that the presented VCD displays the actual 'state-of-the-art'.

Since the differences between the predictions of the two *ab initio* theories are of the same order compared with experiment, it is not possible to give preference to one of them on this level. To avoid a mixing of theory and experiment during the data processing, experimental conditions such as temperature vibration and anomalous dispersion should be included directly into the computer code for calculating (*ab initio*) theoretical structure factors.

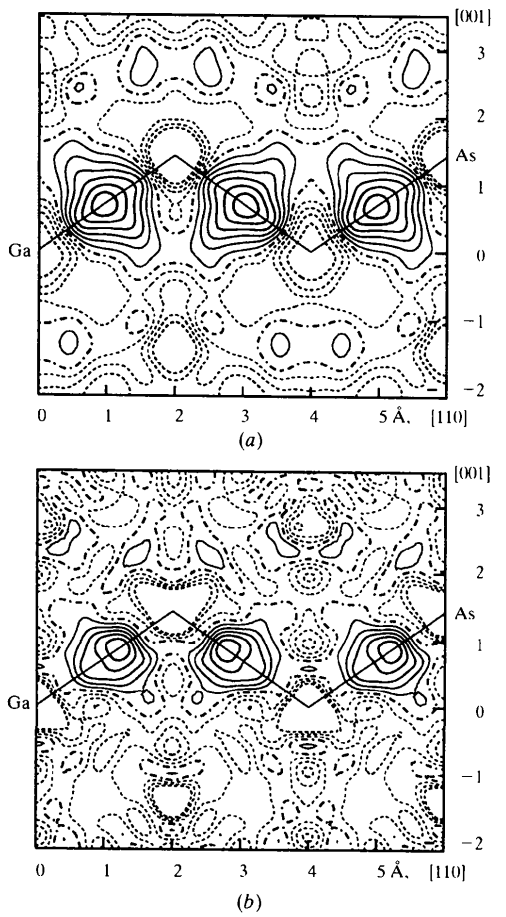

Fig. 6. DCD, calculated from (*a*) experimental and (*b*) theoretical (HF) structure factors after subtraction of F^{sph} (all taken from Table 3). The distance between the contour lines is 0.04 e Å^{-3}; negative areas dashed.

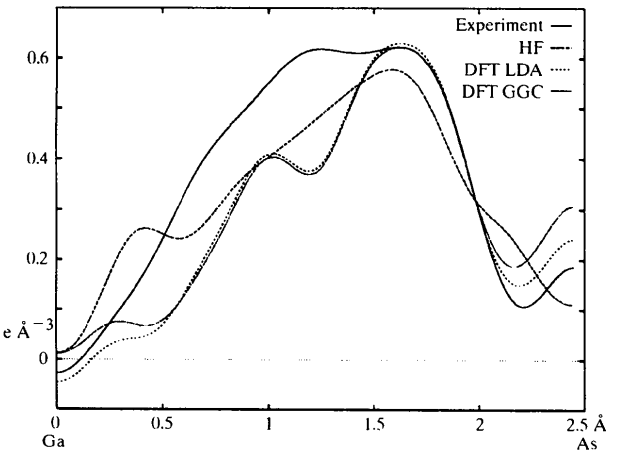

Fig. 7. Cuts through the VCD's obtained from experimental data and theoretical calculations.

The authors thank K. Eichhorn and H.-G. Krane (HASYLAB) for experimental assistance and P. Blaha (Wien) for supplying the theoretical F^{DF}. The thickness measurements were performed at the BAM Berlin. This work was supported by the BMBF (grant 05 647IPA) and the European Community (grant CHRX-CT93-0155).

References

Bilderback, D. H. (1975). Thesis. Purdue University, Indiana, USA.

Blaha, P. (1996). Private communication. Information on *Wien*92 is available at http://info.tuwien.ac.at/theochem/.

Creagh, D. C. (1996). Private Communication.

Cromer, D. T. & Liberman, D. (1970). *J. Chem. Phys.* **53**, 1891–1898.

Dovesi, R., Saunders, V. R. & Roetti, C. (1992). *CRYSTAL92 User's Manual*. University of Torino.

Kato, N. (1968). *J. Appl. Phys.* **39**, 2225–2237.

Kobayshi, K., Takama, T. & Sato, S. (1988). *Jpn. J. Appl. Phys.* **27**, 1377–1380.

Levalois, M. & Allais, G. (1986). *Acta Cryst.* B**42**, 442–449.

Lichanot, A., Azavant, P. & Pietsch, U. (1996). *Acta Cryst.* B**52**, 586–595.

Matsushita, T. & Hayashi, J. (1977). *Phys. Status Solidus A*, **41**, 139–145.

Möhle, M. (1997). Thesis. University of Potsdam, Germany.

Pietsch, U. (1981). *Phys. Status Solidus B*, **103**, 93–100.

Pietsch, U. & Hansen, N. K. (1996). *Acta Cryst.* B**52**, 596–604.

Pietsch, U., Paschke, K. & Eichhorn, K. (1993). *Acta Cryst.* B**49**, 822–825.

Pietsch, U., Tsirelson, V. G. & Ozerov, V. G. (1986). *Phys. Status Solidus B*, **138**, 47–52.

Saravanan, R., Mohanlal, S. K. & Chandrasekaran, K. S. (1992). *Acta Cryst.* A**48**, 4–9.

Stevenson, A. W. (1994). *Acta Cryst.* A**50**, 621–632.

Stevenson, A. W. (1996). *Acta Cryst.* A**52**, C-355.

Su, Z. & Coppens, P. (1994). Sagamore XI. Extended Abstracts P4-16, p. 198.

Towler, M. (1996). *Private Communication.* Further Gauss basis sets for *CRYSTAL* are available at http://gserv1.dl.ac.uk/TCSC/staff/Harrison_N_M/crystal.

Willis, B. T. M. (1969). *Acta Cryst.* A**24**, 277–300.

Zachariasen, W. H. (1967). *Acta Cryst.* **23**, 558–564.